Hybrid NMPC Applied to a Solar-powered Membrane Distillation System

Juan D. Gil [*] **Paulo R.C. Mendes** [***] **G. A. Andrade** [***]
Lidia Roca [**] **Julio E. Normey-Rico** [***] **Manuel Berenguel** [*]

[*] *Centro Mixto CIESOL, ceiA3, Universidad de Almería. Ctra. Sacramento s/n, Almería 04120, Spain; {juandiego.gil,beren}@ual.es.*
[**] *CIEMAT-Plataforma Solar de Almería, Ctra. de Senés s/n, Tabernas 04200, Almería, Spain; lidia.roca@psa.es*
[***] *Federal University of Santa Catarina, Department of Automation and Systems, Florianpolis, Brazil; {paulo.mendes,gustavo.artur, julio.normey}@ufsc.br*

Abstract: This work proposes a hybrid control strategy for the optimal operation of a solar membrane distillation facility. This kind of plants presents a hybrid nature allowing their operation in several modes, which must be properly selected according to the operating conditions. Thus, the control algorithm is based on a mixed logical dynamical characterization of the solar membrane distillation facility, combined with the application of a practical nonlinear model predictive control strategy for calculating the optimal control actions. The main objectives of the control system are to increase the operating temperature and the distillate production of the membrane distillation module, as well as the number of operational hours. For these goals, the control algorithm has to select the most appropriate operating mode and the optimal operating points in terms of water flow rate at each sampling time. Simulation results are presented for evidencing the benefits of the proposed control approach.

Keywords: Mixed Logical Dynamical Systems, Model Predictive Control, Solar Energy, Desalination.

1. INTRODUCTION

Solar Membrane Distillation (SMD) is an under investigated separation technology, suitable for developing self-sufficient plants to be used in applications like desalting sea or brackish water (Zaragoza et al., 2014). However, despite the promising features of the technology (Alkhudhiri et al., 2012), it has not been industrially implemented so far, being the combination with solar energy one of the main barriers. The unpredictable nature of solar energy requires intermittent operations, as well as the use of adequate storage devices. From the control point of view, SMD facilities can be considered as hybrid systems that can be modeled using the Mixed Logical Dynamical (MLD) framework, thus requiring suitable hybrid control strategies for optimal performance.

Most of the papers related to automatic control of SMD processes propose low level control strategies. Such strategies are based on simple control loops, composed by Proportional Integral (PI) or On/Off controllers (Chang et al., 2012; Gil et al., 2018b), which have as main objective to maintain desired temperature setpoints in some parts of the facility at hand. A more advanced control strategy was proposed in Porrazzo et al. (2013), in which a real time optimization approach dealing with the maximization of the distillate production according to operating conditions was presented. Nevertheless, these control techniques do not take into account the hybrid nature of SMD facility operations, which could be very relevant to reduce thermal energy losses in the solar field, and to increase the distillate production. A first step towards the hybrid consideration of a SMD facility was presented in the previous work Gil et al. (2018a), in which three operating modes were considered, defining deterministic rules to make the change between them, and using a Practical Nonlinear Model Predictive Controller (PNMPC) strategy for the optimal operation of each mode.

In this work, an improvement of the approach presented in Gil et al. (2018a) is presented, by considering the SMD facility as a MLD system, and developing a hybrid PNMPC strategy that provides the optimal control actions at each sampling time, which can be stated as a Mixed Integer Linear Programming (MILP) problem. This fact allows us to consider the hybrid nature of the facility in the formulation of the control problem, taking into account the changes among the different operating modes presented in the plant along the control horizon. The objectives of the control system are to maximize the number of operational hours of the facility, the operating temperature and the distillate production of the Membrane Distillation (MD) module. For these goals, five operating modes were defined, which are included in the optimization problem by means of operational constraints. The control system selects the operating mode and the optimal operating points in

⋆ This work has been funded by the National R+D+i Plan Projects DPI2014-56364-C2-1/2-R and DPI2017-85007-R of the Spanish Ministry of Economy, Industry and Competitiveness and ERDF funds, and by projects CNPq 305785/2015-0 and 401126/2014-5.

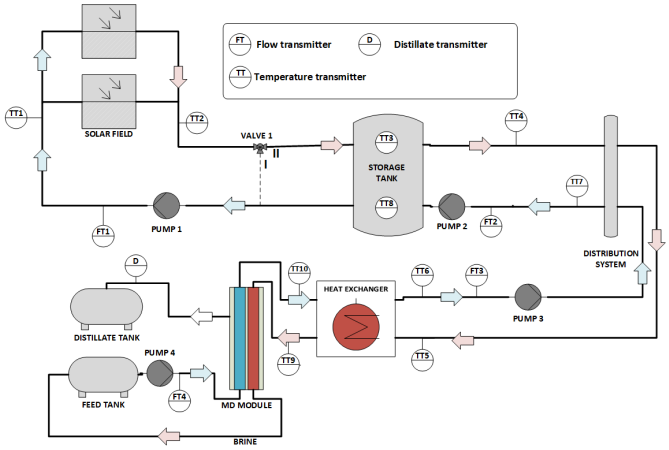

Fig. 1. Schematic diagram of the solar membrande distillation facility.

terms of flow rates at each sampling time, according to the operating conditions. Simulation results are shown to evidence the control system performance. In addition, a comparison with the operation with a rule based controller is provided.

2. SOLAR MEMBRANE DISTILLATION FACILITY

The facility used as reference in this work is located in Plataforma Solar de Almería and it was fully described in Zaragoza et al. (2014).

2.1 MLD System modeling

The complete model of the SMD facility was already developed and validated in Gil et al. (2018a,b,c). For this reason, and due to the lack of space, only a simplified model of the system is presented in this work, in order to highlight the MLD characterization of the plant.

The temperature at the outlet of the solar field was modeled with a lumped-parameters model, which can be described in a simplified way as

$$\mathrm{TT2} = f_2(\mathrm{I}(t), \mathrm{T}_a(t), \mathrm{TT1}(t), \delta_1(t) \cdot \mathrm{FT1}(t)), \quad (1)$$

where $f_2(\cdot)$ is a function of its arguments, I is the global irradiance (W/m^2), T_a is the ambient temperature (^{o}C), and δ_1 is a binary variable related with the logic state of pump 1 (δ_1=0 when the pump is turned off and δ_1=1 when pump 1 is turned on). The rest of variables are according to Fig. 1. It should be mentioned that, in order to eliminate the discontinuity, the term $\delta_1 \cdot$ FT1 in eq. (1) has been replaced by an auxiliary continuous variable z_1 by using the methodology presented in Bemporad and Morari (1999) (Big-M method) for transforming logic propositions in linear inequalities, satisfying that $[\delta_1{=}0]{\rightarrow}[z_1{=}0]$, $[\delta_1{=}1]{\rightarrow}[z_1{=}\mathrm{FT1}]$.

The inlet temperature of the solar field can be modeled with a static model based on the mix produced in valve 1 (see Fig. 1):

$$\mathrm{TT1}(t) = \mathrm{TT2}(t) \cdot (1 - \delta_2(t)) + \mathrm{TT8}(t) \cdot \delta_2(t), \quad (2)$$

where δ_2 is equal to 0 when valve 1 is in position I (see Fig. 1), and equal to 1 when the valve 1 is in position II (see Fig. 1).

A two-nodes stratified dynamic model was used for the storage tank, which is described by

$$\mathrm{TT3} = f_3(\mathrm{TT2}(t), \mathrm{TT8}(t), \mathrm{T}_a(t), \delta_1(t){\cdot}\delta_2(t){\cdot}\mathrm{FT1}(t), \delta_3(t){\cdot}\mathrm{FT2}(t)), \quad (3)$$

$$\mathrm{TT8} = f_8(\mathrm{TT3}(t), \mathrm{TT7}(t), \mathrm{T}_a(t), \delta_1(t){\cdot}\delta_2(t){\cdot}\mathrm{FT1}(t), \delta_3(t){\cdot}\mathrm{FT2}(t)), \quad (4)$$

where δ_3 is a logic variable equal to 0 when pump 2 is turned off, and equal to 1 when pump 2 is turned on. Notice that the term $\delta_1{\cdot}$FT1 in eqs. (3)-(4) can be replaced by the auxiliary variable z_1 previously defined. So, following the Big-M framework, a new variable z_2 is defined for eliminating the discontinuity $\delta_2{\cdot}z_1$. In the same way, another auxiliary variable z_3 replacing the term $\delta_3{\cdot}$FT2 in eq. (4) has been introduced.

The outlet temperatures at both sides of the heat exchanger were characterized with a first principles static model:

$$\mathrm{TT6} = f_6(\mathrm{TT5}(t), \mathrm{TT10}(t), \delta_4(t){\cdot}\mathrm{FT3}(t), \delta_5(t){\cdot}\mathrm{FT4}(t)), \quad (5)$$

$$\mathrm{TT9} = f_9(\mathrm{TT10}(t), \mathrm{TT5}(t), \mathrm{TT6}_m(t), \delta_4(t){\cdot}\mathrm{FT3}(t), \delta_5(t){\cdot}\mathrm{FT4}(t)), \quad (6)$$

where $\mathrm{TT6}_m$ is the temperature calculated in eq. (5), and δ_4 and δ_5 are logic variables associated with the discrete states of pumps 3 and 4, which are equal to 0 when pumps are turned off and equal to 1 when pumps are turned on. As in the previous cases, the terms $\delta_4{\cdot}$FT3 and $\delta_5{\cdot}$FT4 in eqs. (5) and (6) have been replaced by two new auxiliary variables z_4 and z_5 following the Big-M methodology.

Finally the distillate production (D) of the MD module was modelled by means of a Multi-Layer Feedforward Neural Network (Gil et al., 2018c):

$$\mathrm{D} = f_{\mathrm{D}}(\mathrm{TT9}(t), \delta_5(t) \cdot \mathrm{FT4}(t), \mathrm{T}_{feed}(t), \mathrm{S}(t)), \quad (7)$$

where T_{feed} is the temperature of the feed water (fixed at 20 ^{o}C), and S the feed water salinity (fixed at 35 g/L). In the same way, the temperature at the outlet of the condenser channel of the MD module was modelled with a static model that depends on the same variables:

$$\mathrm{TT10} = f_{10}(\mathrm{TT9}(t), \delta_5(t) \cdot \mathrm{FT4}(t), \mathrm{T}_{feed}(t), \mathrm{S}(t)). \quad (8)$$

It should be pointed out that the term $\delta_5{\cdot}$FT4 in eqs. (7) and (8) has been also replaced by the auxiliary variable z_5.

2.2 System operating modes

The system operating modes can be defined from valve 1 position and pumps 1, 2, 3 and 4 discrete states. The relation between the five operating modes used in this work and the values of the variables associated with the discrete states of actuators are presented in table 1. Besides, Fig. 2 shows the logic relations between modes.

In mode 1, the objective is to augment the outlet solar field temperature. This mode is activated as long as the global irradiance is higher than a determined value I^*, and TT2≥TT1. The second mode is devoted to increase the temperature of the tank, and it is used when the outlet solar field temperature is higher than that of the tank (TT2≥TT3), and the temperature in the tank does not allow to operate the MD module over 60 °C, which is the lower limit of the MD module temperature operating range (Zaragoza et al., 2014). Once the temperature in the tank permits operating the MD unit over 60 °C, the mode 3 can be used. In this mode the tank feeds the MD module, and the solar field is used to increase the thermal energy stored in the tank. Mode 4 is used when the MD module can be fed by the tank, but the solar field cannot be run due to the condition TT2≤TT1, and the irradiance value is lower than I^*. Mode 5 is similar to the mode 4, but in this case, the irradiance is higher than I^*, and TT2≥TT1, therefore the solar field can be operated. However, TT2≤TT3, so that, the fluid is recirculated trough the solar field until reaching the temperature in the tank (TT3). It should be commented that mode 0 is the initial state of the plant. Note that the facility is always started up in similar conditions, due to the fact that at the end of the operation the tank approximately maintains the same conditions that at the beginning, because of the temperature operational range of the MD module.

Mode	δ_1	δ_2	δ_3	δ_4	δ_5
0. Initial state	0	0	0	0	0
1. Solar field	1	0	0	0	0
2. Solar tank load	1	1	0	0	0
3. Solar tank load and MD	1	1	1	1	1
4. Tank unload and MD	0	V*	1	1	1
5. Solar field, tank unload and MD	1	0	1	1	1

Table 1. System operating modes. V* means that in mode 4, valve 1 could be in positions I or II, depending on the previous mode.

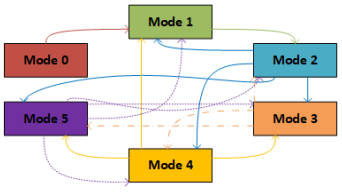

Fig. 2. Relations between operating modes. All the modes can return to mode 0, however the joints have been omitted for the sake of simplicity.

3. CONTROL SYSTEM DEVELOPMENT

The control strategy developed in this work has three main objectives: i) to extend the number of operational hours of the system by increasing the thermal energy stored in the buffer system; ii) to maximize the operating temperature of the MD module, what implies an enhancement of the thermal efficiency of the process (Gil et al., 2018a); and iii) to increase the distillate production of the MD module. In this sense, the control system has to select the most appropriate operating mode and calculate the optimal operating points in terms of flow rate for each pump at each sampling time. The following subsections show the development of the control system.

3.1 Practical Nonlinear Model Predictive Control technique

The PNMPC strategy was proposed by Plucenio et al. (2007), and it uses an approximation for representing an output prediction vector, $\hat{\mathbf{Y}}$, along a determined prediction horizon, N, as a linear function of the future control actions, $\Delta\mathbf{u}$:

$$\hat{\mathbf{Y}} = \mathbf{F} + \mathbf{G} \cdot \mathbf{\Delta u}. \tag{9}$$

where $\hat{\mathbf{Y}}=[\hat{Y}(t|t)...\hat{Y}(t+N|t)]^T$ *, $\mathbf{F}=[\hat{F}(t|t)...\hat{F}(t+N|t)]^T$, $\mathbf{\Delta u}=[\Delta u(t|t)...\Delta u(t+N_c\text{-}1|t)]^T$, N_c is the control horizon, and matrix $\mathbf{G}$ is the Jacobian matrix $\frac{\partial \hat{\mathbf{Y}}}{\partial \mathbf{\Delta u}}$ calculated in the operating point u. In this technique, the free response $\mathbf{F}$ is calculated with the nonlinear model of the system (Plucenio et al., 2007; Gil et al., 2018a). In this work, this strategy is used to compute the prediction of TT2, TT3, TT9 and D.

On the one hand, the prediction of TT2 ($\hat{\mathbf{Y}}_{\mathbf{TT2}}$) is a function of past inputs $\mathbf{z_1}$, past outputs $\mathbf{TT2}$, and future control increments $\mathbf{\Delta z_1}=\boldsymbol{\delta_1}\cdot\mathbf{\Delta FT1}$, so that, following the PNMPC procedure it can be calculated as:

$$\hat{\mathbf{Y}}_{\mathbf{TT2}} \approx \mathbf{F}_{\mathbf{TT2}} + \mathbf{G_1} \cdot \mathbf{\Delta z_1}, \tag{10}$$

where $\mathbf{G_1}$ is the Jacobian matrix $\frac{\partial \hat{\mathbf{Y}}_{\mathbf{TT2}}}{\partial \mathbf{\Delta z_1}}$,

In the same way, the prediction of TT3 ($\hat{\mathbf{Y}}_{\mathbf{TT3}}$) can be calculated as $\hat{\mathbf{Y}}_{\mathbf{TT3}} = f(\mathbf{TT3}, \mathbf{z_2}, \mathbf{z_3}, \mathbf{\Delta z_2}, \mathbf{\Delta z_3})$:

$$\hat{\mathbf{Y}}_{\mathbf{TT3}} \approx \mathbf{F}_{\mathbf{TT3}} + [\mathbf{G_2}\ \mathbf{G_3}] \cdot [\mathbf{\Delta z_2}; \mathbf{\Delta z_3}], \tag{11}$$

where $\mathbf{\Delta z_2}=\boldsymbol{\delta_2}\cdot\mathbf{\Delta z1}$, $\mathbf{\Delta z_3}=\boldsymbol{\delta_3}\cdot\mathbf{\Delta FT2}$, $\mathbf{G_2}$ is the jacobian $\frac{\partial \hat{\mathbf{Y}}_{\mathbf{TT3}}}{\partial \mathbf{\Delta z_2}}$, and $\mathbf{G_3}$ the Jacobian matrix $\frac{\partial \hat{\mathbf{Y}}_{\mathbf{TT3}}}{\partial \mathbf{\Delta z_3}}$.

On the other hand, the prediction of TT9 ($\hat{\mathbf{Y}}_{\mathbf{TT9}}$) can be calculated as a function of past outputs $\mathbf{TT9}$, past inputs $\mathbf{z_3}, \mathbf{z_4}, \mathbf{z_5}$, and future control actions $\mathbf{\Delta z_3}, \mathbf{\Delta z_4}, \mathbf{\Delta z_5}$. Nevertheless, FT3 is operated at the same value that FT4 (z_4=z_5) to achieve the maximum thermal transference in the heat exchanger, as was experimentally established in Gil et al. (2018a). Therefore, $\hat{\mathbf{Y}}_{\mathbf{TT9}}$ can be computed in a simplified way as follows:

$$\hat{\mathbf{Y}}_{\mathbf{TT9}} \approx \mathbf{F}_{\mathbf{TT9}} + [\mathbf{G_4}\ \mathbf{G_5}] \cdot [\mathbf{\Delta z_3}; \mathbf{\Delta z_5}], \tag{12}$$

where $\mathbf{\Delta z_5}=\boldsymbol{\delta_5}\cdot\mathbf{\Delta FT4}$, and $\mathbf{G_4}$ and $\mathbf{G_5}$ are the Jacobian matrices $\frac{\partial \hat{\mathbf{Y}}_{\mathbf{TT9}}}{\partial \mathbf{\Delta z_3}}$, and $\frac{\partial \hat{\mathbf{Y}}_{\mathbf{TT9}}}{\partial \mathbf{\Delta z_5}}$ respectively.

Finally, the prediction of the distillate production ($\hat{\mathbf{Y}}_{\mathbf{D}}$) can be calculated as:

$$\hat{\mathbf{Y}}_{\mathbf{D}} \approx \mathbf{F}_{\mathbf{D}} + \mathbf{G_6} \cdot \mathbf{\Delta z_5}, \tag{13}$$

* The nomenclature $\hat{x}(t+j|t)$ means the value of the variable $\hat{x}$ at the instant time $t+j$, calculated with the information acquire up in instant t.

$\mathbf{G_6}$ is the Jacobian matrix $\frac{\partial \hat{\mathbf{Y}}_{\mathbf{D}}}{\partial \mathbf{\Delta z_5}}$,

It should be remarked that, the advantage of using the PNMPC strategy is that the dependence of predictions to the manipulated variables are linear along the horizon, allowing to formulate the optimization problem concerning this work as a MILP problem. Moreover, this technique has been complemented with a method for predicting the global irradiance (Pawlowski et al., 2011) in order to improve the predictions.

3.2 Objective function

The cost function used in this work is composed by four main terms (see eq. (14)), which are employed to achieve the proposed objectives of the control architecture, and due to the fact that the plant can be run in several modes with different associated objectives.

$$\begin{aligned} J = &- \gamma_1 \cdot \sum_{k=1}^{N} (\mathrm{v}(t+k|t) + \mathrm{w}(t+k|t)) \\ &- \gamma_2 \cdot \sum_{k=1}^{N} \hat{\mathrm{Y}}_{\mathrm{TT9}}(t+k|t) - \gamma_3 \cdot \sum_{k=1}^{N} \hat{\mathrm{Y}}_{\mathrm{D}}(t+k|t) \\ &+ \gamma_4 \cdot \sum_{k=1}^{N_c} \cdot \sum_{i=1}^{5} |\Delta z_i(t+k-1|t)|, \end{aligned} \tag{14}$$

where γ_1, γ_2, γ_3, and γ_4 are weighting factors. In addition, it should be commented that, due to the differences in magnitude of the terms involved in the objective function, they have been normalized.

To augment the number of operational hours of the system, the thermal energy stored in the tank must be maximized. To do this, the first term of the objective function is composed by two objectives, which are changed according to the operating mode. When the facility runs in modes 1 or 5, in which the fluid is recirculated trough the solar field (valve 1 in position I in Fig. 1), the objective consists on maximizing the temperature at the outlet of the solar field, trying to reach the temperature at the top of the tank as fast as possible to start loading it. Once the temperature at the top of the tank is reached, and the operating mode is changed, the objective is to increase TT3. To introduce this proposition in the objective function, three new auxiliary variables have been defined. The first one consists on a logic variable $\boldsymbol{\delta}_{\mathbf{aux,1}}$, which is introduced by the following constraints:

$$\boldsymbol{\delta}_{\mathbf{aux,1}} + \boldsymbol{\delta}_{\mathbf{2}} \leq \mathbf{1}, \quad \boldsymbol{\delta}_{\mathbf{aux,1}} + \boldsymbol{\delta}_{\mathbf{2}} \geq \mathbf{0}, \tag{15}$$

where $\boldsymbol{\delta}_{\mathbf{aux,1}}$=$[\delta_{aux,1}(t|t)...\delta_{aux,1}(\mathrm{t}+N_c\text{-}1|t)]^T$, and $\boldsymbol{\delta}_{\mathbf{2}}$ = $[\delta_2(t|t)...\delta_2(\mathrm{t}+N_c\text{-}1|t)]^T$, and $\mathbf{1}$ is a vector of ones of length N_c. This statement implies that $[\boldsymbol{\delta}_{\mathbf{aux,1}}\mathbf{=0}]\rightarrow[\boldsymbol{\delta}_{\mathbf{2}}\mathbf{=1}]$, $[\boldsymbol{\delta}_{\mathbf{aux,1}}\mathbf{=1}]\rightarrow[\boldsymbol{\delta}_{\mathbf{2}}\mathbf{=0}]$, where $\mathbf{0}$ is a vector of zeros of length N_c. The other two auxiliary variables can be defined as $\mathbf{v}$=$\boldsymbol{\delta}_{\mathbf{aux,1}}\cdot\hat{\mathbf{Y}}_{\mathbf{TT2}}$, and $\mathbf{w}$=$\boldsymbol{\delta}_{\mathbf{2}}\cdot\hat{\mathbf{Y}}_{\mathbf{TT3}}$ and introduced in the problem by means of the Big-M methodology. The second and the third term of the objective function are aimed at maximizing the operating temperature (TT9 in Fig. 1) and the distillate production (D) of the MD module. The last term is devoted to penalize the control efforts as they have associated economical costs.

3.3 Process constraints

Since the fluid of the heat generation circuit is demineralized water, the temperature should be lower than 100 °C to avoid the creation of vapour. In the same way, the temperature at the inlet of the MD module cannot be higher than 80 °C due to the thermal limit of membrane materials (Zaragoza et al., 2014). So, the following constraints have been added:

$$\hat{\mathbf{Y}}_{\mathbf{TT2}} \leq 100, \hat{\mathbf{Y}}_{\mathbf{TT3}} \leq 100, \hat{\mathbf{Y}}_{\mathbf{TT9}} \leq 80. \tag{16}$$

In addition, the physical limits of the pumps must be taken into account. The maximum and minimum flow rate value provided by each pump are:

$$7{\leq}\mathrm{FT1}{\leq}20, \quad 15{\leq}\mathrm{FT2}{\leq}25, \quad 7{\leq}\mathrm{FT3}{\leq}10, \quad 7{\leq}\mathrm{FT4}{\leq}10, \tag{17}$$

where the values are in L/min. Notice that these values have been taken into account for defining z_1, z_3, z_4 and z_5 with the Big-M formulation.

3.4 Operational constraints

In this subsection, the constraints used for activating o deactivating the pumps of the facility, and for opening and closing valve 1 are shown. Notice that the operating modes are defined according to the discrete states of actuators (δ_1, δ_2, δ_3, δ_4 and δ_5), as was established in section 2.2. Thus, the constraints developed in this section are used to represent the physical requirements of the operation of the plant, following the relationships presented in Fig. 2.

Firstly, to activate δ_1, two conditions have to be satisfied. The first one is related with the irradiance level, so that, the solar field can only be turned on when I^* is reached. Thus, considering k=1, ..., N_c, this condition can be described by the following constraints:

$$\begin{aligned} &\hat{I}(t+k|t) - \delta_{aux,2}(t+k\text{-}1|t) \cdot I^* \geq 0 + \epsilon_1, \\ &(1 - \delta_{aux,2}(t+k\text{-}1|t)) \cdot \hat{I}(t+k|t) - I^* \leq 0 + \epsilon_2, \end{aligned} \tag{18}$$

where $\hat{I}(t+1|t)...\hat{I}(t+N_c|t)$ are the predicted values obtained by the irradiance forecasting method, and $\delta_{aux,2}$ is an auxiliary logic variable. Notice that the first constraint ensures that $[\delta_{aux,2}(t+k\text{-}1|t)=1]\rightarrow[\hat{I}(t+k|t) \geq I^*]$ and the second one that $[\delta_{aux,2}(t+k\text{-}1|t)=0]\rightarrow[\hat{I}(t+k|t) \leq I^*]$.

On the other hand, the second condition used for activating/deactivating δ_1 is in charge of ensuring that the solar field is turned on as long as the outlet solar field temperature is higher than the inner one, thus avoiding thermal losses:

$$\begin{aligned} &\hat{\mathrm{Y}}_{\mathrm{TT2}}(t+k|t) - \delta_{aux,3}(t+k\text{-}1|t) \cdot \mathrm{TT1}(t|t) \geq 0 + \epsilon_3, \\ &(1 - \delta_{aux,3}(t+k\text{-}1|t)) \cdot \hat{\mathrm{Y}}_{\mathrm{TT2}}(t+k|t) - \mathrm{TT1}(t|t) \leq 0 + \epsilon_4, \end{aligned} \tag{19}$$

where $\delta_{aux,3}$ is also an auxiliary logic variable. As happened in the previous case, the first constraint ensures that $[\delta_{aux,3}(t+k\text{-}1|t)=1]\rightarrow[\hat{\mathrm{Y}}_{\mathrm{TT2}}(t+k|t) \geq \mathrm{TT1}(t|t)]$ and the second one that $[\delta_{aux,3}(t+k\text{-}1|t)=0]\rightarrow[\hat{\mathrm{Y}}_{\mathrm{TT2}}(t+k|t) \leq \mathrm{TT1}(t|t)]$. It should be noted that the second constraint in eq. (19) can be rewritten as:

$$\begin{aligned} &(1 - \delta_{aux,3}(t+k\text{-}1|t)) \cdot (\sum_{i=1}^{N_c} \frac{\delta \hat{\mathrm{Y}}_{\mathrm{TT2}}(t+k|t)}{\delta \Delta z_1(t+i\text{-}1|t)} \cdot \\ &\cdot \Delta z_1(t+i\text{-}1|t) + F(t+k|t)) - \mathrm{TT1}(t|t) \leq 0 + \epsilon_4, \end{aligned} \tag{20}$$

so, as it can be observed, there is a bilinear term ($\delta_{aux,3}{\cdot}z_1$) in the constraint. However, considering the case in which $\delta_{aux,3}(t{+}k\text{-}1|t){=}0$, $\hat{\mathrm{Y}}_{\mathrm{TT2}}(t{+}k|t)$ is equal to the free response, and considering $\delta_{aux,3}(t{+}k\text{-}1|t){=}1$, the term $(1\text{-}\delta_{aux,3}(t{+}k\text{-}1|t))\hat{\mathrm{Y}}_{\mathrm{TT2}}(t{+}k|t)$ is zero. So that, the constraint can be formulated as:

$$(1-\delta_{aux,3}(t{+}k\text{-}1|t))\cdot F(t{+}k|t)-\mathrm{TT1}(t|t)\leq 0+\epsilon_4. \quad (21)$$

In this way, the value of $\boldsymbol{\delta_1}{=}[\delta_1(t+k-1|t)...\delta_1(t+N_c-1|t)]^T$ is calculated as $\boldsymbol{\delta_1}{=}\boldsymbol{\delta_{aux,2}}\cdot\boldsymbol{\delta_{aux,3}}$, which can be introduced in the optimization problem by using the Big-M framework.

Secondly, the following proposition has been formulated for opening valve 1 (position II in Fig. 1), $[\delta_2{=}1]{\leftrightarrow}[\mathrm{TT2}{\geq}\ \mathrm{TT3}]$, which can be introduced as:

$$\begin{aligned}&(1-\delta_2(t{+}k\text{-}1|t))\cdot\hat{\mathrm{Y}}_{\mathrm{TT2}}(t{+}k|t)-\hat{\mathrm{Y}}_{\mathrm{TT3}}(t{+}k|t)\leq 0+\epsilon_5,\\&\hat{\mathrm{Y}}_{\mathrm{TT2}}(t{+}k|t)-\delta_2(t{+}k\text{-}1|t)\cdot\hat{\mathrm{Y}}_{\mathrm{TT3}}(t{+}k|t)\geq 0+\epsilon_6.\end{aligned} \quad (22)$$

As in the previous cases, two constraints have been used, the first one ensures that $[\delta_2(t{+}k\text{-}1|t){=}0]\ \rightarrow\ [\hat{\mathrm{Y}}_{\mathrm{TT2}}(t{+}k|t)\leq\hat{\mathrm{Y}}_{\mathrm{TT3}}(t{+}k|t)]$, and the second one ensures $[\delta_2(t{+}k\text{-}1|t){=}1]\rightarrow[\hat{\mathrm{Y}}_{\mathrm{TT2}}(t{+}k|t)\geq\hat{\mathrm{Y}}_{\mathrm{TT3}}(t{+}k|t)]$. If these two constraints are rewritten in the form of eq. (20), some bilinear terms can be observed, which are $\delta_2{\cdot}z_1$, $\delta_2{\cdot}z_2$, and $\delta_2{\cdot}z_3$. Therefore, three new real variables have been defined for replacing them, $\mathbf{q}{=}\boldsymbol{\delta_2}{\cdot}\mathbf{z_1}$, $\mathbf{r}{=}\boldsymbol{\delta_2}{\cdot}\mathbf{z_2}$, and $\mathbf{s}{=}\boldsymbol{\delta_2}{\cdot}\mathbf{z_3}$, which are introduced by means of the Big-M methodology in the optimization problem. Thus, eq. (22) can be rewritten as:

$$\begin{aligned}&\sum_{i=1}^{N_c}\frac{\delta\hat{\mathrm{Y}}_{\mathrm{TT2}}(t{+}k|t)}{\delta\Delta z_1(t{+}i\text{-}1|t)}\cdot(\Delta z_1(t{+}i\text{-}1|t)-\Delta\mathrm{q}(t{+}i\text{-}1|t))+\\&+(1-\delta_2(t{+}k\text{-}1|t))\cdot F(t{+}k|t))-\hat{\mathrm{Y}}_{\mathrm{TT3}}(t{+}k|t)\leq 0+\epsilon_5,\\&\hat{\mathrm{Y}}_{\mathrm{TT2}}(t{+}k|t)-(\sum_{i=1}^{N_c}\frac{\delta\hat{\mathrm{Y}}_{\mathrm{TT3}}(t{+}k|t)}{\delta\Delta z_2(t{+}i\text{-}1|t)}\cdot\Delta\mathrm{r}(t{+}i\text{-}1|t)+\\&+\sum_{i=1}^{N_c}\frac{\delta\hat{\mathrm{Y}}_{\mathrm{TT3}}(t{+}k|t)}{\delta\Delta z_3(t{+}i\text{-}1|t)}\cdot\Delta\mathrm{s}(t{+}i\text{-}1|t)+\\&+\delta_2(t{+}k\text{-}1|t)\cdot F(t{+}k|t))\leq 0+\epsilon_6,\end{aligned} \quad (23)$$

Finally, δ_3, δ_4 and δ_5 are turned to 0 or 1 according to the value of a new logic auxiliary variable $\delta_{aux,4}$, which satisfies that $[\delta_{aux,4}{=}1]{\leftrightarrow}[\mathrm{TT3}{\geq}\mathrm{T}^*]$, where T^* is the required temperature in the tank for operating the MD module over 60 °C. This temperature can be computed at each sampling time as $\mathrm{T}^*(t){=}60\ ^\circ\mathrm{C}{+}\Delta\mathrm{T}_{he}(t)$, where $\Delta\mathrm{T}_{he}(t)$ is the temperature difference of the heat exchanger, which can be calculated with the model of the heat exchanger (Gil et al., 2018a). Thus, the following constraints have been formulated:

$$\begin{aligned}&\hat{\mathrm{Y}}_{\mathrm{TT3}}(t{+}k|t)-\delta_{aux,4}(t{+}k\text{-}1|t)\cdot\mathrm{T}^*(t|t)\geq 0+\epsilon_7,\\&(1-\delta_{aux,4}(t{+}k\text{-}1|t))\cdot\hat{\mathrm{Y}}_{\mathrm{TT3}}(t{+}k|t)-\mathrm{T}^*(t|t)\leq 0+\epsilon_8.\end{aligned} \quad (24)$$

It should be noted that the first constraint ensures that $[\delta_{aux,4}(t{+}k\text{-}1|t){=}1]\ \rightarrow\ [\hat{\mathrm{Y}}_{\mathrm{TT3}}(t{+}k|t)\ \geq\ \mathrm{T}^*(t|t)]$, and the second one that $[\delta_{aux,4}(t{+}k\text{-}1|t){=}0]\ \rightarrow\ [\hat{\mathrm{Y}}_{\mathrm{TT3}}(t{+}k|t)\ \leq\ \mathrm{T}^*(t|t)]$. Again, the second constraint can be rewritten in the form of eq. (20). However, in this case, only one auxiliary real variable has to be used for replacing the bilinear term $\delta_{aux,4}{\cdot}z_2$. This variable is defined as $\mathbf{x}{=}\boldsymbol{\delta_{aux,4}}{\cdot}\mathbf{z_2}$, and introduced in the optimization problem by means of the Big-M methodology. In this way, the constraint can be rewritten as:

$$\begin{aligned}&\sum_{i=1}^{N_c}\frac{\delta\hat{\mathrm{Y}}_{\mathrm{TT3}}(t{+}k|t)}{\delta\Delta z_2(t{+}i\text{-}1|t)}\cdot(\Delta z_2(t{+}i\text{-}1|t)-\Delta\mathrm{x}(t{+}i\text{-}1|t))+\\&+(1-\delta_{aux,4}(t{+}k\text{-}1|t)\cdot F(t{+}k|t))-\mathrm{T}^*(t|t)\leq 0+\epsilon_8.\end{aligned} \quad (25)$$

It should be commented that $\boldsymbol{\epsilon}{=}[\epsilon_1,...,\epsilon_8]$ is a slack variable used to avoid infeasible solutions when the constraints are equal to 0. This variable is also penalized in the objective function with a term $10^5\cdot\boldsymbol{\epsilon}$. Notice also that these kind of constraints can produce chattering problems, however, the predictions have been filtered using the mean values of the three previous sampling times, to avoid it.

4. RESULTS AND DISCUSSION

The control strategy has been tested in simulation (using the nonlinear dynamical model of the facility as real plant). Illustrative results are presented in this section using meteorological data from PSA on the day March 6, 2017. The sampling time used was 5 min, selected taking into account the system dynamics. N was fixed at 6, due to the reliability of the irradiance forecasting method (30 min), and N_c at 3, following traditional recommendations in MPC strategies, $N_c \ll N$. The values of the weighting factors were γ_1=0.3, γ_2= 0.3, γ_3=0.4, and γ_4=0.1 selected after systematic simulations until obtaining the desired closed loop performance, and the value of I^* was fixed at 150 W/m^2 since lower values do not help to increase the temperature in the solar field. To solve the optimization problem the software Matlab, with Yalmip toolbox and solver CPLEX, has been used. Besides the initial conditions in the tank were established at 57 and 56 °C for TT3 and TT8 respectively.

Fig. 3 presents representative results. When the estimated global irradiance value is higher than 150 W/m^2 and the estimated TT2 is higher than TT1, the controller activates mode 1, until reaching the temperature at the top of the tank (8.15 h), instant in which the controller changes to mode 2. In mode 1, FT1 is operated at its minimum value for increasing TT2, then, in mode 2, FT1 is run at its maximum value thus increasing TT3. At time instant 8.25 h, the controller closes valve 1 due to irradiance disturbances, and then, after three sample times it opens valve 1 again (mode 2). Mode 3 is activated at time instant 10.20 h. It can be observed that at 13.50 h, due to irradiance fluctuations, the controller decreases FT1 during two sample times. Finally, around 16.00 h, the controller changes between modes 5 and 3 several times, trying to continue loading the tank. Finally, the controller selects mode 4 until the end of the operation, maintaining FT4 at its maximum value for enhancing the distillate production (Gil et al., 2018a,c).

To evidence the advantages of considering the changes between modes in the prediction horizon and calculating the optimal flow rate setpoints at each sample time, the results have been compared with an operation with a rule based

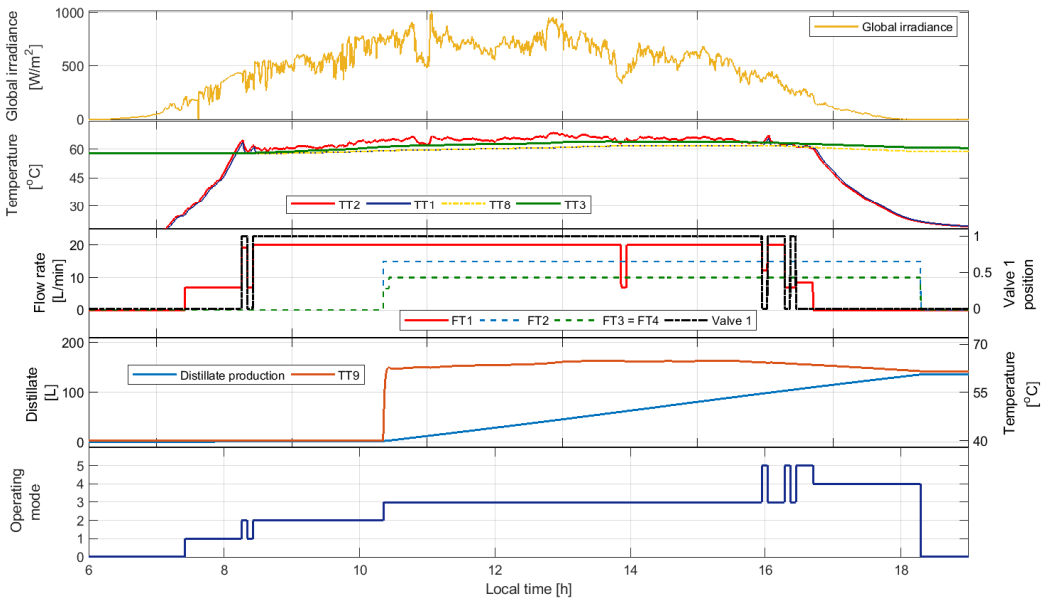

Fig. 3. Simulation results. All the variables are according to Fig. 1

Controller	Distillate [L]	Operating hours [h]	$TT9_{max}$ [°C]
Rule based	137.90	7.16	64.13
HPNMPC	139.60	7.97	64.90

Table 2. Comparison between results. HPNMPC is Hybrid PNMPC controller.

controller with fixed flow rate setpoints. This controller was configured using the same conditions as in the hybrid PNMPC technique for changing between modes, and using flow rates similar as the ones provided by the hybrid PNMPC technique in each mode. However, is this controller the conditions are checked with actual values, instead of estimated ones. The results are quantitatively presented in Tab. 2. As can be observed, the hybrid controller extends the operations around 50 min more than the rule based one. This fact together with the increase of TT9 cause that the distillate production augments.

5. CONCLUSIONS

This paper has addressed the development of a hybrid NMPC controller for a SMD plant. The controller showed satisfactory performance, managing in an optimal way the changes between the different operating modes, and providing optimal flow rates according to the operating conditions at each sample time. A comparison between the proposed strategy and a state machine based operation was carried out, showing an enhancement of the distillate production of 1.40 % and an extension of the operational hours of around 11 %. Notice that the algorithm has been applied in simulation in a small pilot plant, in industrial cases the improvements achieved (in absolute terms) could be very relevant in the daily operation.

REFERENCES

Alkhudhiri, A., Darwish, N., and Hilal, N. (2012). Membrane distillation: a comprehensive review. *Desalination*, 287, 2–18.

Bemporad, A. and Morari, M. (1999). Control of systems integrating logic, dynamics, and constraints. *Automatica*, 35(3), 407–427.

Chang, H., Lyu, S.G., Tsai, C.M., Chen, Y.H., Cheng, T.W., and Chou, Y.H. (2012). Experimental and simulation study of a solar thermal driven membrane distillation desalination process. *Desalination*, 286, 400–411.

Gil, J.D., Roca, L., Ruiz-Aguirre, A., Zaragoza, G., and Berenguel, M. (2018a). Optimal operation of a solar membrane distillation pilot plant via nonlinear model predictive control. *Computers & Chemical Engineering*, 109, 151–165.

Gil, J.D., Roca, L., Zaragoza, G., and Berenguel, M. (2018b). A feedback control system with reference governor for a solar membrane distillation pilot facility. *Renewable Energy*, 120, 536–549.

Gil, J.D., Ruiz-Aguirre, A., Roca, L., Zaragoza, G., and Berenguel, M. (2018c). Prediction models to analyse the performance of a commercial-scale membrane distillation unit for desalting brines from RO plants. *Desalination*, 445, 15–28.

Pawlowski, A., Guzmán, J.L., Rodríguez, F., Berenguel, M., and Normey-Rico, J.E. (2011). Predictive control with disturbance forecasting for greenhouse diurnal temperature control. *IFAC Proceedings Volumes*, 44(1), 1779–1784.

Plucenio, A., Pagano, D., Bruciapaglia, A., and Normey-Rico, J. (2007). A practical approach to predictive control for nonlinear processes. *IFAC Proceedings Volumes*, 40(12), 210–215.

Porrazzo, R., Cipollina, A., Galluzzo, M., and Micale, G. (2013). A neural network-based optimizing control system for a seawater-desalination solar-powered membrane distillation unit. *Computers & Chemical Engineering*, 54, 79–96.

Zaragoza, G., Ruiz-Aguirre, A., and Guillén-Burrieza, E. (2014). Efficiency in the use of solar thermal energy of small membrane desalination systems for decentralized water production. *Applied Energy*, 130, 491–499.